

## Identification of Inhibitors of Inositol 5-Phosphatases through Multiple Screening Strategies

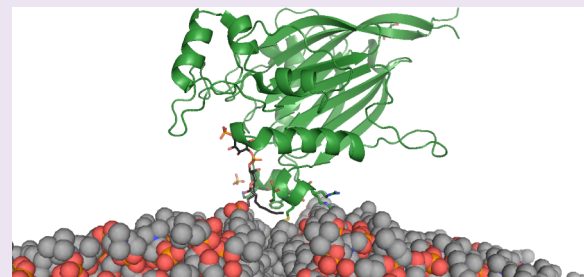
Michelle Pirruccello,<sup>†,§</sup> Ramiro Nandez,<sup>†</sup> Olof Idevall-Hagren,<sup>†,||</sup> Abel Alcazar-Roman,<sup>†</sup> Laura Abriola,<sup>‡</sup> Shana Alexandra Berwick,<sup>†</sup> Louise Lucast,<sup>†</sup> Dayna Morel,<sup>†</sup> and Pietro De Camilli<sup>†,\*</sup>

<sup>†</sup>Department of Cell Biology, Howard Hughes Medical Institute and Program in Cellular Neuroscience, Neurodegeneration and Repair, Yale University School of Medicine, New Haven Connecticut 06510, United States

<sup>‡</sup>Yale Center for Molecular Discovery, Yale University, West Haven, Connecticut 06516, United States

### Supporting Information

**ABSTRACT:** Phosphoinositides are low abundance membrane phospholipids that have key roles in signaling, membrane trafficking, and cytoskeletal dynamics in all cells. Until recently, strategies for robust and quantitative development of pharmacological tools for manipulating phosphoinositide levels have focused selectively on PI(3,4,5)P<sub>3</sub> due to the importance of this lipid in growth factor signaling and cell proliferation. However, drugs that affect levels of other phosphoinositides have potential therapeutic applications and will be powerful research tools. Here, we describe methodology for the high-throughput screening of small molecule modulators of the inositol 5-phosphatases, which dephosphorylate PI(4,5)P<sub>2</sub> (the precursor for PI(3,4,5)P<sub>3</sub>) and PI(3,4,5)P<sub>3</sub>). We developed three complementary *in vitro* activity assays, tested hit compounds on a panel of 5-phosphatases, and monitored efficacy toward various substrates. Two prominent chemical scaffolds were identified with high nanomolar/low micromolar activity, with one class showing inhibitory activity toward all 5-phosphatases tested and the other selective activity toward OCRL and INPPSB, which are closely related to each other. One highly soluble OCRL/INPPSB-specific inhibitor shows a direct interaction with the catalytic domain of INPPSB. The efficacy of this compound in living cells was validated through its property to enhance actin nucleation at the cell cortex, a PI(4,5)P<sub>2</sub> dependent process, and to inhibit PI(4,5)P<sub>2</sub> dephosphorylation by OCRL (both overexpressed and endogenous enzyme). The assays and screening strategies described here are applicable to other phosphoinositide-metabolizing enzymes, at least several of which have major clinical relevance. Most importantly, this study identifies the first OCRL/INPPSB specific inhibitor and provides a platform for the design of more potent inhibitors of this family of enzymes.



Phosphoinositide (PI) lipids derive from the phosphorylation of phosphatidylinositol at the 3, 4, and 5 positions of the inositol ring resulting in the generation of seven phosphoinositide species with differing localization and functions within cells. Dynamic control of their levels and of their heterogeneous distribution within cellular membranes is achieved through the actions of an array of kinases, phosphatases, and phospholipases. Aberrant phosphoinositide metabolism underlies several pathological conditions,<sup>1</sup> most notably cancer, given the key role of PI(3,4,5)P<sub>3</sub> in cell growth and proliferation. Accordingly, enzymes controlling the levels of PI(3,4,5)P<sub>3</sub> are an important therapeutic target.<sup>2</sup> Other therapeutic uses of drugs directed against PI metabolizing enzymes have been recently suggested.<sup>3–6</sup>

One important class of PI metabolizing enzymes are inositol 5-phosphatases. Members of this protein family play a major role in the control of PI(4,5)P<sub>2</sub>, a PI that resides primarily, although not exclusively, on the cytoplasmic leaflet of the plasma membrane. Via direct interactions of its phosphorylated headgroup, this phospholipid has a broad range of actions, including effects on signaling scaffolds, ion channel function,

exo-endocytosis, the actin cytoskeleton, and thus cell polarity and migration. Impaired spatiotemporal control of PI(4,5)P<sub>2</sub> has been implicated in several leukemias, metabolic disorders, neurodegenerative diseases, and genetic disorders.<sup>7,8</sup> Additionally, PI(4,5)P<sub>2</sub> is the precursor of other important signaling molecules, such as IP<sub>3</sub> (inositol triphosphate, a soluble phosphoinositol), via the action of phospholipase C and PI(3,4,5)P<sub>3</sub> via the action of PI 3-kinases. Both IP<sub>3</sub>, as well as other inositolpolyphosphates (IPs) and PI(3,4,5)P<sub>3</sub> are also substrates of 5-phosphatases, so that this class of enzymes has a multiplicity of key physiological functions.

There are 10 mammalian enzymes with a conserved inositol 5-phosphatase domain. Each enzyme has unique substrate preferences, IPs, PI(4,5)P<sub>2</sub>, or PI(3,4,5)P<sub>3</sub>, with one enzyme, INPPSA (also called type I inositol 5-phosphatase) selectively acting on IPs.<sup>9</sup> Additionally, each family member has a specific pattern of tissue distribution and subcellular localization

**Received:** March 1, 2014

**Accepted:** April 17, 2014

**Published:** April 17, 2014

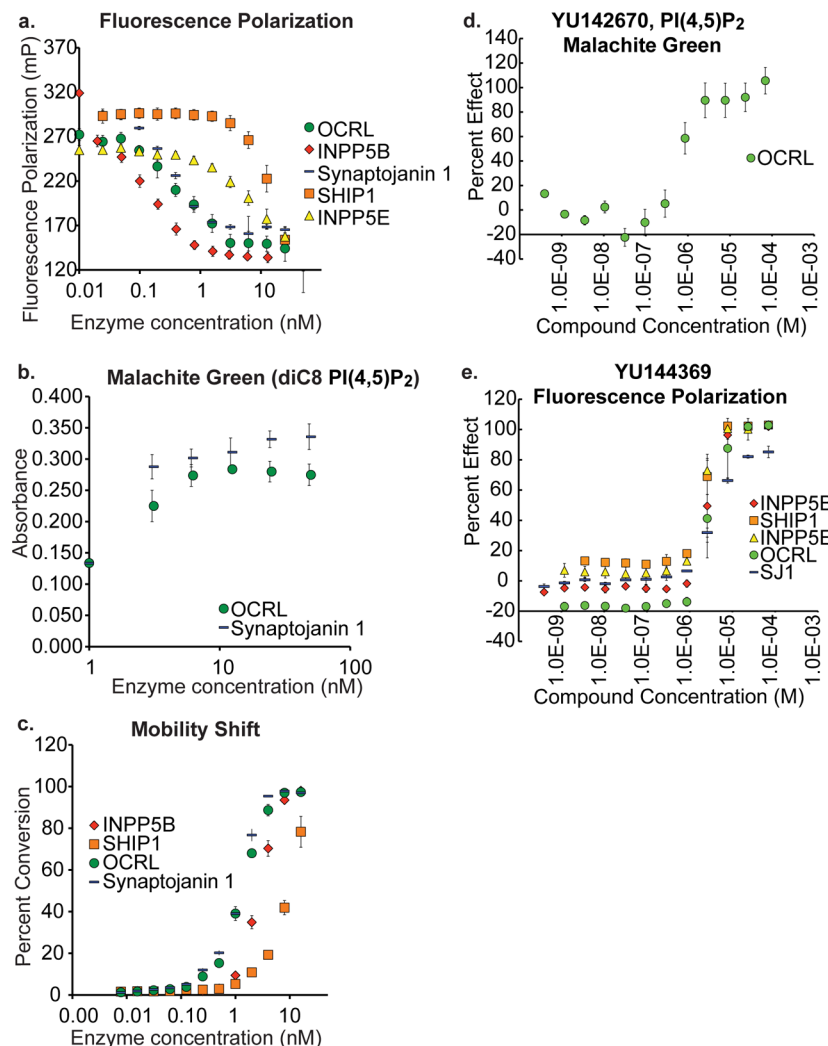


**Figure 1.** Representative data showing enzyme titration at constant substrate concentration for (a) the fluorescence polarization (FP) assay, 2.5  $\mu$ M PI(3,4,5)P<sub>3</sub>; (b) the malachite green (MG) assay (25  $\mu$ M PI(4,5)P<sub>2</sub>); and (c) the mobility shift (MS) assay (500 nM PI(3,4,5)P<sub>3</sub>). (d and e) Representative 12 point dose response curves for (d) YU142679 in the malachite green assay and (e) YU144369 in the fluorescence polarization assay. All data was measured in quadruplicate; errors indicate the standard deviation.

(reflecting unique sets of protein–protein interactions and preferential actions on specific PI pools). Thus, these enzymes display both unique and partially overlapping functions.

Current methods for studying specific 5-phosphatases rely primarily upon genetic models, overexpression, chronic enzyme depletion (by knockdown or knockout methods), or changes arising from spontaneous mutations in human patients or model organisms. These methods, however, are susceptible to compensatory mechanisms. Thus, the availability of small compounds for the selective and acute manipulation of endogenous 5-phosphatase activities, and possibly of specific member(s) of this protein family, would represent a powerful tool for basic research. These compounds could also have important therapeutic applications.<sup>7,8</sup>

Assays toward the development of specific small molecule modulators of 5-phosphatases have been reported, and some of them have led to the isolation of SHIP1 and SHIP2 inhibitors and activators,<sup>5,10–13</sup> but no inhibitors with selectivity for other members of the 5-phosphatase family have been described.

Here, we describe a screening strategy for the identification of small molecule modulators of 5-phosphatases. The initial high-throughput screens focused on identifying synaptjanin 1

and OCRL modifiers. Synaptjanin 1 is the major 5-phosphatase of synapses.<sup>14,15</sup> OCRL is a ubiquitously expressed 5-phosphatase whose loss of function results in OculoCerebroRenal Syndrome of Lowe, a condition involving renal tubular dysfunction, developmental delay/intellectual disability, and congenital cataracts. Candidate compounds were then assayed for their activity toward other inositol 5-phosphatases: INPP5B, a close homologue of OCRL, and the more structurally divergent phosphatases SHIP2, INPP5E, and INPP5A. Inhibitory effectiveness on 5-phosphatase activity using different substrates, such as diC16 PI(4,5)P<sub>2</sub>, diC8 PI(3,4,5)P<sub>3</sub>, and IP3 was also analyzed.

As a result of this comprehensive screening strategy, which could be extended to the isolation of modulators of other PI modifying enzymes, we have identified a small molecule inhibitor with specificity for OCRL/INPP5B over the enzymes tested in our panel and verified the efficacy of this compound in three separate assays in living cells.

## RESULTS AND DISCUSSION

### High Throughput Screening and Assay Development.

We developed three different assay formats for screening

compound libraries. These assays were complementary to each other, and the combination of three separate assays allowed us to exclude false-positive hits due to assay interference. Importantly, this strategy also allowed us to test efficacy of our compounds against phosphoinositides with differences in both their lipid chain (IP<sub>3</sub>, diC<sub>8</sub>, diC<sub>16</sub>) and degree of phosphorylation.

Our main tool for the screening of 5-phosphatase activity was a competitive fluorescence polarization (FP) assay that detects the conversion of PI(3,4,5)P<sub>3</sub> into PI(3,4)P<sub>2</sub>, using a GST-tagged TAPP1 PH domain as a detector for PI(3,4)P<sub>2</sub>. Specifically, dephosphorylation of diC<sub>8</sub> PI(3,4,5)P<sub>3</sub> produced excess, unlabeled, diC<sub>8</sub> PI(3,4)P<sub>2</sub>, which competitively displaced a trace amount of BODIPY TMR-PI(3,4)P<sub>2</sub> pre-bound to the TAPP1 PH domain.<sup>16</sup> This assay was very sensitive and highly reproducible with Z' scores ranging 0.6–0.9 (a score of 0.5–1 indicates an excellent screening assay). Representative data from this assay is shown in Figure 1a. Representative data from this assay is shown in Figure 1a.

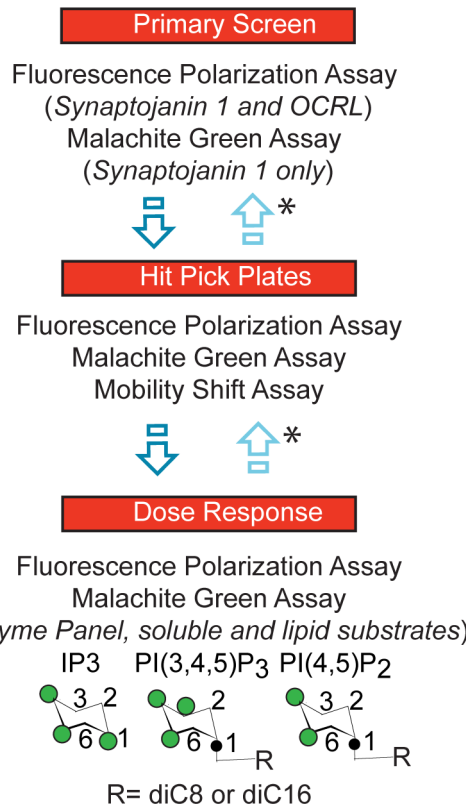
Results from the FP assay were complemented by a malachite green assay (Z' scores 0.5–0.8), which was significantly less sensitive but had the advantage of flexibility in the substrate used (diC<sub>8</sub> PI(4,5)P<sub>2</sub> in our initial screening, also used subsequently for diC<sub>16</sub> PI(4,5)P<sub>2</sub> and IP<sub>3</sub>) (Figure 1b). Finally, a mobility shift (MS) assay monitored the conversion of fluorescein-tagged substrate (either PI(4,5)P<sub>2</sub> or PI(3,4,5)P<sub>3</sub>) using a combination of capillary electrophoresis and microfluidics<sup>13</sup> (Figure 1C, Z' scores 0.5–0.7). This assay effectively removed signal contributions from compounds and reduced assay interference. However, dose response analysis in this assay was hindered by the speed of the detection step. Thus, this assay was primarily utilized to confirm hits from the other assays.

Our overall screening strategy is outlined in Scheme 1. Using a combination of the FP and malachite green assays, a total of 37 579 compounds were screened in 384 well format for activity toward Synaptojanin 1. The FP assay was used exclusively to screen for OCRL modifiers in 384 well format with a total of 29 087 compounds tested. We choose a hit enrichment boundary of 3 standard deviations away from the median percent effect, and with this boundary we had a hit rate of 0.56–1.8%. Hit pick plates, with 320 (Synaptojanin 1) and 298 (OCRL) compounds were then tested with both enzymes, since each enzyme was screened independently with partially overlapping libraries. We found 33 compounds with significant activity in the OCRL hit pick screens and 76 compounds with significant activity in the Synaptojanin 1 hit pick screen.

Compounds were further characterized with dose response. Many of the compounds identified in the OCRL and Synaptojanin hit pick screens overlapped. Thus, for the dose response curves we picked 36 compounds which had either (1) activity toward both OCRL and Synaptojanin or (2) activity in two of our activity assays (22 for OCRL and 21 for Synaptojanin). We also included a known SHIP2 inhibitor as a negative control.<sup>12</sup> We initially measured 4 point curves with 36 compounds, of which 12 displayed inhibitory activity toward OCRL in both the malachite green and fluorescence polarization assays, and 10 displayed inhibitory activity toward Synaptojanin in the same two assays (Supporting Information (SI) Table 1). After the 4 point dose response, we followed up with a 12 point curve with the 12 best candidates. See Figure 1d, e for representative 12 point dose response curves.

Our top compounds fell within the acceptable range for Lipinski's rule of five for druglike properties (Figure 2a). All

### Scheme 1. Schematic of Our Screening Strategy<sup>a</sup>



<sup>a</sup>\* denotes places where structure–activity relationship (SAR)-directed iterations occurred.

were less than 500 Da, carried less than 5 hydrogen bond donors and less than 10 hydrogen bond acceptors, and had calculated partition coefficient (LogP) values ranging 0.7–5. However, many of the top hits were not soluble in aqueous solution, hampering their further characterization. Thus, we explored related compounds with enhanced solubility for activity in our assays. Structure activity relationship (SAR) analysis of the top compounds from both dose response and primary screening data prompted us to screen all other compounds in the available libraries with chemical similarity. We identified eight major scaffold classes among the screen positives (see SI Figure 1). Compounds with significant activity were further characterized by dose response, and the process was iterated several times.

This iterative optimization process quickly showed that members of only the first two scaffold classes, Class I and Class II, produced multiple hits with favorable qualities. Criteria included reproducible IC<sub>50</sub> values of less than 10 μM, saturating dose response curves with maximal percent effects that reached >90%, and a Hill coefficient that is close to 1 (a steep dose response curve can indicate compound aggregation). In fact, even in the first 36 compound dose response analysis, one can see an enrichment of compounds belonging to Class I and II. In total, we identified 13 compounds containing a triazolo[3,4-b][1,3,4]thiadiazole with substitutions at the 3 and 6 positions that were grouped into Class I. Class II compounds, which comprised 24 members, contained a core benzyl amine group (see SI Figure 1).

The three top compounds from Class I and Class II are illustrated in Figure 2A. IC<sub>50</sub> values were in the low

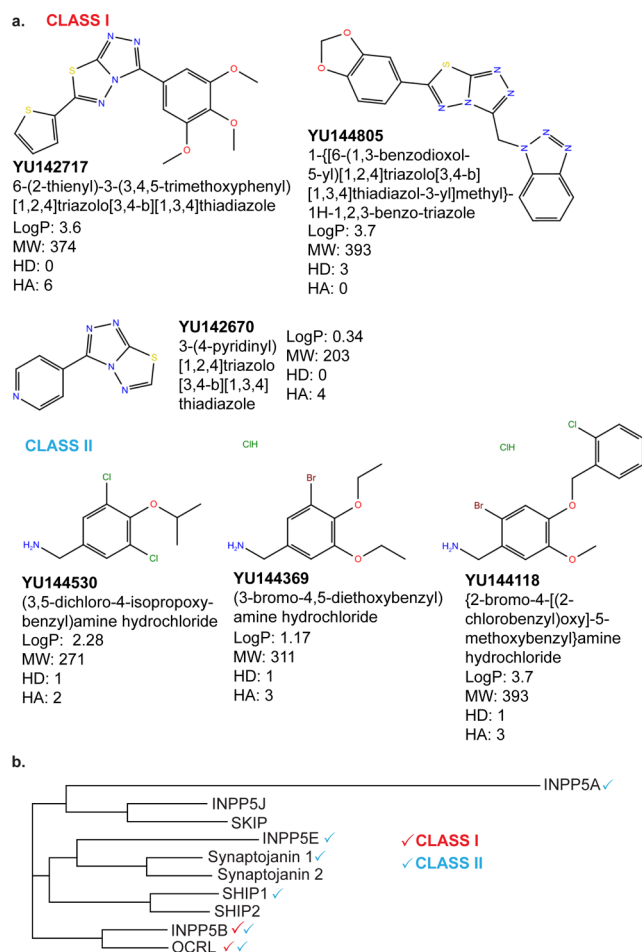


**Figure 2.** Two main scaffold classes and their distinctive activities toward the inositol 5-phosphatases. (a) Three top compounds in each class are shown. (b) Phylogenetic dendrogram of the inositol 5-phosphatase domains of the 10 mammalian family members. Red and blue check marks next to enzyme names denotes sensitivity to Class I (red) or Class II (blue) compounds.

micromolar to high nanomolar range (Table 1). To our knowledge, none of the identified compounds have structural similarity to currently identified 5-phosphatase modifiers.

We were particularly interested in YU142670 because of its chemical similarity to molecules in one of our main scaffold classes (Class I) along with a favorable calculated LogP value (0.34), predicting better solubility. Interestingly, YU142670, was present in our initial high-throughput screening but was not identified as a hit due to interference in the FP assay (Table 1), which manifested as high background fluorescence values. When measured by dose response in the FP assay, this interference shifted the apparent percent effects of the compound in the dose response curves. Even with this background, saturating dose-dependent inhibition of enzyme activity by this compound was measured for OCRL and INPP5B (although it did not reach 80% effect) and not other family members tested (either no response, or a small response at very high concentrations of the compound)(see also below).

To gain a more accurate measurement of the IC<sub>50</sub> we measured the dose response curve for YU142670 in the malachite green assay with diC16 PI(4,5)P<sub>2</sub> as a substrate (Figure 1D). In this assay, we reached 100% effect on OCRL and INPP5B activity with an IC<sub>50</sub> of 0.71 and 1.78 μM, respectively (Table 1). Thus, given its favorable chemical properties, this compound became our lead compound for measurement of binding affinity by Isothermal Titration Calorimetry and for several assays to test efficacy in cell culture (see below).

As negative controls, we analyzed efficacy toward two unrelated phosphatases: Shrimp Alkaline phosphatase (SAP), a general phosphatase which can also act on nucleic acids, and Phosphatase and TENSin homologue (PTEN), a PI(3,4,5)P<sub>3</sub> 3-phosphatase. No representatives from the two main scaffold classes displayed significant inhibitory activity toward these enzymes, shown in Table 1. A third enzyme, neutral bacterial sphingomyelinase, which shares a similar fold to the inositol 5-phosphatases (a DNase I fold), was also tested. This enzyme was not sensitive to any Class I compounds screened. Results with Class II compounds were not conclusive due to assay interference (compounds caused a signal increase, which resulted in negative, compound concentration-dependent, percent effects).

**Selectivity within the 5-Phosphatase Family.** The core of the Inositol 5-phosphatase domain consists of 11 β-strands mainly running antiparallel to each other, forming 2 β-sheets

**Table 1. Activity from Dose Response Curves of Top Compounds in the Two Identified Classes<sup>a</sup>**

enzyme	assay	substrate	Class I			Class II		
			YU142670	YU142717	YU144805	YU144369	YU144530	YU144118
SJ1	FP	PI(3,4,5)P <sub>3</sub>	none	none	none	3.63	>70	1.3
OCRL	FP	PI(3,4,5)P <sub>3</sub>	1.32 <sup>b</sup>	2.98	1.56	3	3.59	4.59
INPP5B	FP	PI(3,4,5)P <sub>3</sub>	17.5 <sup>b</sup>	39.01	10.38	2.55	3	3.97
SHIP1	FP	PI(3,4,5)P <sub>3</sub>	none	none	none	2.52	2.89	8.97
INPP5E	FP	PI(3,4,5)P <sub>3</sub>	>70 <sup>b</sup>	none	>70	2.33	2.8	5.77
INPPSA	malachite	IP3	none	none	>70	1.07	1.44	1.81
INPPSB	malachite	IP3	0.53	0.92	0.57	0.57	0.81	1.1
OCRL	malachite	PI(4,5)P <sub>2</sub>	0.71	0.68	0.86	3.61	5.77	4.06
INPP5B	malachite	PI(4,5)P <sub>2</sub>	1.78	2.63	1.39	1.65	2.6	2.24
<sup>c</sup> SAP	malachite	dNTPs	ND	none	none	>50	>50	>50
PTEN	mobility shift	PI(3,4,5)P <sub>3</sub>	ND	none	none	ND	ND	none
sphingomyelinase	fluorescence	sphingomyelin	none	none	>70	none <sup>b</sup>	none <sup>b</sup>	none <sup>b</sup>

<sup>a</sup>Average IC<sub>50</sub> values from lead compounds, in μM. Unless otherwise indicated data are from 12 point dose response curves with 4 replicates. ND: not determined. None: no impact on activity at any compound concentration tested. >50 or >70, less than 50% impact on activity was detected at highest doses of compound, either 50 or 70 μM. <sup>b</sup>Assay interference detected. <sup>c</sup>Data from a 4 point dose response curve.

surrounded by a layer of  $\alpha$ -helices.<sup>17,18</sup> The active site sits in a relatively shallow pocket formed by the tips of the  $\beta$ -strands at one pole of the module (SI Figure 2), which shares several common features among family members.<sup>18</sup> The active site geometry is held in place by the core fold of the protein, which can withstand some variability in its sequence while maintaining the correct secondary structure. Thus, members of the 5-phosphatase family have the same basic enzymatic function while displaying quite distinct amino acid sequences, as revealed by sequence identities for the human 5-phosphatase domains ranging from 15–60% (sequence homology is ~30–70%) (see SI Table 3). Differences in the regions surrounding the active site likely help determine substrate specificity.<sup>7</sup> The relatedness of the catalytic domains of the human inositol 5-phosphatases is depicted in a phylogenetic dendrogram in Figure 2b.

In order to assess the specificity of our compounds toward various members of the 5-phosphatase family, we tested the compounds toward other members of this family that can act on PIs: INPP5B, SHIP1 and INPP5E. INPP5B is the closest homologue to OCRL, with 69% homology in the catalytic domain. We chose SHIP1 and INPP5E as our other control enzymes due to their clinical relevance<sup>8</sup> and their sequence diversity within the family. The IC<sub>50</sub> values for representatives from our lead scaffold classes are indicated in Table 1. Assessment of the activity of these enzymes in dose response curves shows that while Class II compounds inhibit all 5-phosphatases in the panel, no inhibition was detected when Synaptojanin, SHIP1, or INPP5E were assayed with the Class I compounds (see Figure 2c for a summary).

Note that our original screening assays utilized either full length OCRL, or a construct of Synaptojanin-1 containing the Sac1 and 5-phosphatase domains. When we tested efficacy of these compounds toward INPP5B we used a construct comprising only the 5-phosphatase domain. The finding that both compounds classes displayed activity toward the INPP5B catalytic domain indicates that they act on the 5-phosphatase domain (Table 1) (see also below).

We also tested our lead compounds in 5-phosphatase assays (malachite assays) with IP<sub>3</sub> as the substrate. IP<sub>3</sub> is the precursor of other inositol polyphosphates and of pyrophosphates, the molecules that result from the reversible phosphorylation and pyrophosphorylation of the inositol ring (by well over 25 mammalian enzymes), to generate 13 species with important signaling functions. We included in this assay INPP5A, the only 5-phosphatase that acts exclusively on IPs, while the other 9 members of the 5-phosphatase family act on both IP<sub>3</sub> and PIs with varied efficacy. The identification of small molecules that selectively interfere with either lipid or soluble substrates would be useful research and therapeutic tools with potentially fewer off-target effects.

Consistent with previous reports, we found that INPP5B (here the catalytic domain) displayed robust activity against IP<sub>3</sub>, whereas OCRL had barely detectable activity at high enzyme concentrations (SI Figure 3).<sup>19,20</sup>

Importantly, using IP<sub>3</sub> as the substrate, as shown in Table 1, we found significant inhibitory activity of both compounds toward the catalytic domain of INPP5B (IC<sub>50</sub> values ranging 0.5–1.1  $\mu$ M). The same scaffold class with inhibitory activity toward OCRL, INPP5B, Synaptojanin 1, INPP5E, and SHIP1 (Class II) also showed dose-dependent activity against INPP5A, while the Class I compounds did not inhibit INPP5A. Altogether, our dose response data suggests that

Class II compounds are pan 5-phosphatase inhibitors whereas the Class I compounds specifically target OCRL and INPP5B.

**Direct Interaction between YU142670 and the INPP5B Catalytic Domain.** We utilized isothermal titration calorimetry (ITC) to measure interactions of the most soluble compounds of each class (YU142670 from Class I, YU144369 from Class II) with the catalytic domain of the OCRL/INPP5B subgroup of 5-phosphatases. More specifically, we used the catalytic domain of human INPP5B due to its robust expression from a bacterial source, which was needed to produce sufficient quantities of protein for the experiments. We detected a specific interaction between the INPP5B catalytic domain and YU142670 ( $K_a = 2.35 \times 10^5 \pm 8.744 \times 10^4$ ) (Figure 3). YU144369 also showed measurable heat of binding, however, protein precipitation during the experiment render these results inconclusive (data not shown).

**Efficacy of YU142670 in Live Cells.** We next explored the effect of these compounds in living cells. Preliminary experiments revealed that YU144369 (Class II) had an acute toxicity on cell cultures. Thus, we focused our analysis on YU142670 (Class I), which shows specificity toward OCRL and INPP5B. Cells defective in OCRL function have been previously reported to exhibit enhanced actin nucleation due to accumulation of PI(4,5)P<sub>2</sub>,<sup>21–23</sup> which is a critical factor for the recruitment of actin nucleating proteins to membranes.<sup>24</sup> Thus, we examined whether inhibition of OCRL/INPP5B by YU142670 had an impact on the organization of the actin cytoskeleton. Toward this aim, we expressed an F-actin reporter, CH<sup>Utrrophin</sup>-mCherry,<sup>25</sup> in wild-type human skin fibroblasts and we assessed actin dynamics by live cell confocal microscopy upon addition of YU142670. This compound was used at a concentration which was approximately 50 fold higher than the biochemically measured IC<sub>50</sub> (pilot experiments showed this concentration did not produce obvious toxicity) to account for potentially incomplete cell penetration of the compound (although lower concentrations of compound did produce a measurable effect, data not shown). Addition of YU142670 in 0.5% DMSO, but not 0.5% DMSO alone, produced, within minutes, an accumulation of F-actin foci at the plasma membrane (Figure 4a and b). The number of foci increased over 12-fold in the presence of YU142670 compared with DMSO controls (Figure 4c–e). Many of them developed into dynamic ruffles or filopodia (Figure 4f). The localization of these foci at PI(4,5)P<sub>2</sub> rich sites was confirmed at the same sites by the increase of fluorescence signal for the co-expressed GFP-PH<sup>PLC $\delta$</sup> , a PI(4,5)P<sub>2</sub> biosensor. It remains unclear whether GFP-PH<sup>PLC $\delta$</sup>  hot spots represent a focal accumulation of PI(4,5)P<sub>2</sub> or a change in membrane geometry induced by actin nucleation, as membrane ruffles/folds result in increased membrane associated signal in the optic path.

To further confirm the effects of YU142670 on the 5-phosphatase catalytic activity of OCRL in cells, we utilized an optogenetic method that allows us to monitor selectively this activity.<sup>26</sup> The method is based on the blue light dependent heterodimerization of a “bait” module (CIBN-CAAX) targeted to the plasma membrane and a light-sensitive cryptochrome module (CRY2) fused to the 5-phosphatase domain of OCRL (CRY2-5-ptaseOCRL). Blue-light illumination causes rapid and reversible binding of CRY2-5-ptaseOCRL to CIBN, thus recruiting the 5-phosphatase to the plasma membrane where it will convert its substrate lipid PI(4,5)P<sub>2</sub> to PI4P. This change can be monitored by the loss of plasma membrane associated fluorescence using iRFP-PH-PLC $\delta$ 1, as a PI(4,5)P<sub>2</sub> reporter.<sup>26</sup>

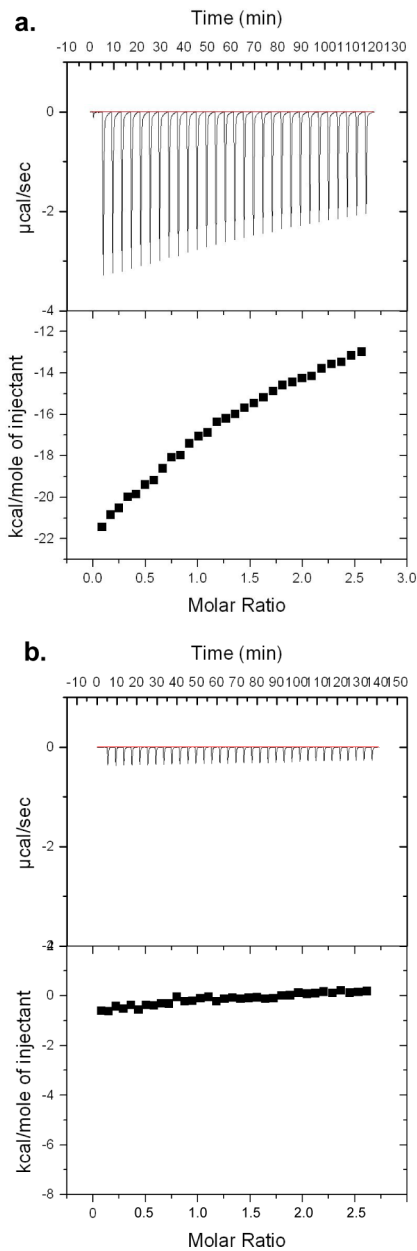


**Figure 3.** Direct interaction of YU142670 with the catalytic domain of INPPSB. (a) ITC trace of YU142670 titration into the catalytic domain of INPPSB shows measurable heat of binding.  $N = 0.9108 \pm 0.0547$ ;  $K_a = 2.352 \times 10^5 \pm 8.744 \times 10^4$ ,  $\Delta H = -7270 \pm 588.6$ ,  $\Delta S = 0.5933$ ,  $\chi^2 = 350238$ . (b) Titration of compound into buffer solution alone.

COS-7 cells expressing CRY2-5-ptaseOCRL, CIBN-CAAX and iRFP-PH-PLC $\delta$ 1 were imaged with TIRF microscopy. In control cells, pre-incubated for 15 min with 0.5% DMSO, blue-light illumination (488-nm, 50 pulses, 200 ms duration, 4 s intervals) delivered through the evanescent field resulted in rapid ( $t_{1/2} = 18 \pm 3$  s,  $n = 14$  cells) and pronounced ( $52 \pm 5\%$ ,  $n = 14$  cells) loss of iRFP-PH-PLC $\delta$ 1 fluorescence, reflecting primarily plasma membrane associated fluorescence (Figure 5a). Interruption of the illumination resulted in redistribution of the biosensor back to the plasma membrane ( $t_{1/2} = 480 \pm 50$  s,  $n = 11$  cells), indicating resynthesis of PI(4,5)P<sub>2</sub>. When the experiment was repeated in the presence of 50  $\mu$ M YU142670 (Figure 5b), blue-light illumination still caused a

rapid ( $t_{1/2} = 25 \pm 4$  s,  $n = 14$  cells) drop in plasma membrane iRFP-PH-PLC $\delta$ 1 fluorescence, but this drop was less pronounced ( $32 \pm 3\%$ ,  $n = 14$  cells,  $P < 0.001$ ). Furthermore, interruption of the illumination resulted in a faster recovery of plasma membrane iRFP-PH-PLC $\delta$ 1 fluorescence ( $t_{1/2} = 180 \pm 23$  s,  $n = 13$  cells,  $P < 0.001$ ) relative to controls, indicating that resynthesis of PI(4,5)P<sub>2</sub> was accelerated compared to control cells. This is consistent with an inhibition of endogenous OCRL.

Finally, we examined the impact of YU142670 on endogenous phosphoinositide levels in human dermal fibroblasts after <sup>3</sup>H-myo-inositol labeling and HPLC analysis of phosphoinositide species. Following a 1 h treatment with 50  $\mu$ M YU142670, increased levels of PI(4,5)P<sub>2</sub>, leading to an increased PI(4,5)P<sub>2</sub>/PI4P ratio, was observed (see Figure 6a for two representative traces and Figure 6b for average ratios). In samples treated with YU142670 ( $n = 6$ ) the PI(4,5)P<sub>2</sub>/PI4P ratio increased 50% (p value of 0.0004) (Figure 6B). All other phosphoinositide levels measured remained unchanged (Figure 6a)

In conclusion, in three separate assay systems, we observe changes in the cortical cytoskeleton, PI(4,5)P<sub>2</sub> biosensor signal, and endogenous PI(4,5)P<sub>2</sub> levels that are consistent with a specific action of this compound on OCRL/INPPSB activity.

**Concluding Remarks.** Here, we describe an efficient method for high-throughput screening of modulators of the inositol 5-phosphatases, and identify a small molecule inhibitor for OCRL and INPPSB. The identification of the first compound with selective activity toward OCRL/INPPSB exemplifies the power of our screening strategy. This inhibitor has modest efficacy, and thus this study is a starting point for the design and selection of more potent inhibitors.

Our strategy utilized three separate assays formats: a fluorescence polarization assay which was highly sensitive but could be biased by compound interference, a much less sensitive malachite green assay, and a mobility shift assay which separated the reaction product from the compound, thus removing artifacts due to compound interference. We leveraged the malachite green and mobility shift assays to detect effects of substrate composition on compound efficacy. In addition, we tested representative members of major structural sub-classes among the 5-phosphatases, thus gaining knowledge of specificity and selectivity, useful information toward reducing potential off-target effects. Importantly, the assays employed in this study could be applied to other phosphoinositide phosphorylating and dephosphorylating enzymes.

We focused our primary screen on Synaptojanin 1 and OCRL, and identified two scaffolds with distinct specificity profiles. The first scaffold was specific for OCRL/INPPSB, with no activity against the other 5-phosphatases tested in this study. A representative compound from this class (YU142670) increased the levels of PI(4,5)P<sub>2</sub> in mouse embryonic fibroblasts or human dermal fibroblasts and inhibited the activity of over-expressed human OCRL in Cos-7 cells.

ITC experiments verified a direct interaction between YU142670 and the catalytic domain of INPPSB. This compound inhibited reactions utilizing all substrates of OCRL and INPPSB, irrespective of lipid chain length or phosphorylation of the 3' position of the inositol ring. Given its effects in cells, it is also inhibitory when OCRL/INPPSB acts on the membrane bilayer. It will be interesting to determine how this compound inhibits enzyme activity, as it likely hits a unique feature of OCRL/INPPSB not present in other 5-

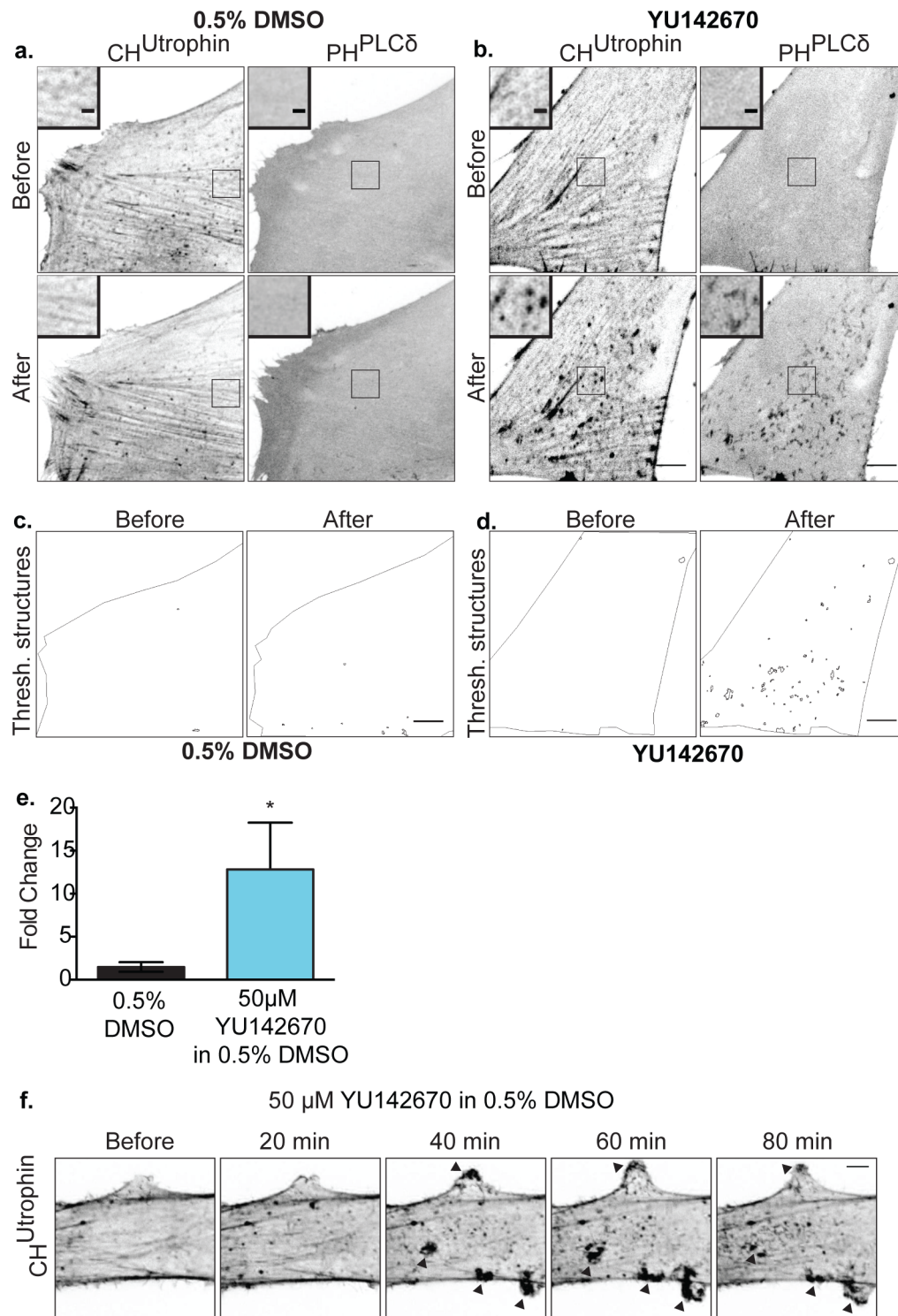


**Figure 4.** YU142670 induces enhanced actin polymerization and ruffle activity at the plasma membrane. (a–b) Confocal micrographs of wild type human fibroblasts expressing CH<sup>Utrophin</sup>-mCherry (left panels) and GFP-PH<sup>PLC $\delta$</sup>  (right panels) before (top panels) and 50 min after (bottom panels) the addition of 0.5% DMSO (A) or 50  $\mu$ M YU142670 in 0.5% DMSO (b). Note the actin (CH<sup>Utrophin</sup>-mCherry) foci that form upon addition of YU142670 and the corresponding modification of GFP-PH<sup>PLC $\delta$</sup>  fluorescence, a marker of PI(4,5)P<sub>2</sub> in the plasma membrane, from a diffuse to a discretely concentrated signal. Spots may represent focal accumulation of PI(4,5)P<sub>2</sub> but also (and more likely) membrane deformations, including ruffles (see field F) induced by the actin foci. Insets show details at higher magnification. These structures were clearly visible within 13 min of YU142670 addition on average ( $\pm 1$ ,  $n = 6$  cells from independent experiments) (Scale bar full frame = 10  $\mu$ m, inset = 2  $\mu$ m). (c–d) Mapping of GFP-PH<sup>PLC $\delta$</sup> -positive spots at the plasma membrane above an arbitrary fluorescence threshold (identical for control and YU142670 treated cells) before (left panels) and 50 min after (right panels) the addition of 0.5% DMSO (c) or 50  $\mu$ M YU142670 (d). (e) Average fold change in the number of GFP-PH<sup>PLC $\delta$</sup> -positive structures at the plasma membrane after thresholding following the addition of 0.5% DMSO (black) or 50  $\mu$ M YU142670 (blue). A greater than 12-fold increase in the number of foci after YU142670 treatment is observed ( $n = 3$  cells from independent experiments;  $p < 0.02$ ). (f) Sequential images of a wild type fibroblast expressing CH<sup>Utrophin</sup>-mCherry before and after the addition of 50  $\mu$ M YU142670. Arrowheads indicate the formation of large dynamic ruffles upon addition of the drug (scale bar = 10  $\mu$ m).

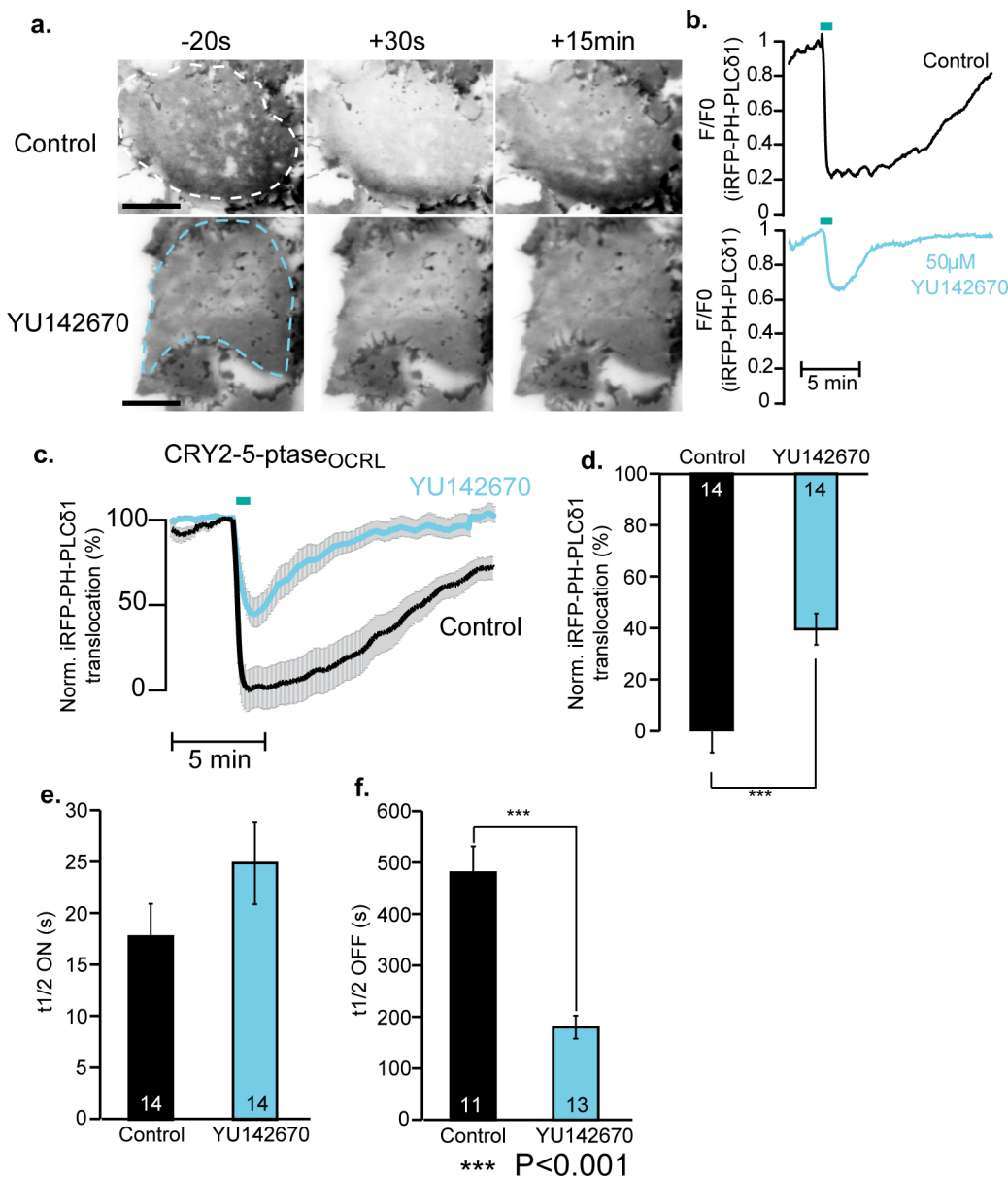


**Figure 5.** YU142670 efficacy *in situ*. (a) Representative timecourse of PI(4,5)P<sub>2</sub> depletion following light-induced recruitment ( $t = 0$  s) of the catalytic domain of OCRL to the plasma membrane of COS-7 cells using a blue light dependent heterodimeric system and iRFP-PH-PLC $\delta$ 1 as a PI(4,5)P<sub>2</sub> reporter (TIRF microscopy). Cells were treated with 0.5% DMSO (control) or 50  $\mu$ M YU142670. Scale bars are 10  $\mu$ M. (b) Example traces are shown for the experiment in a. (c and d) Normalized average traces and maximal translocation from the recording of 14 cells. (e and f)  $t_{1/2}$  of the loss and recovery of PI(4,5)P<sub>2</sub> levels (as detected by iRFP-PH-PLC $\delta$ 1 fluorescence), which are consistent with OCRL inhibition.

phosphatases. Conversely, the second class of compounds inhibited all 5-phosphatases tested and displayed significant cellular toxicity (data not shown).

Modulators of the inositol 5-phosphatases could have diverse applications, both in basic research and in the clinic. Phosphoinositide metabolism is often targeted by pathogens.<sup>27</sup> OCRL and INPP5B reside on the earliest endocytic compartments,<sup>28</sup> and their activity is important, for example, in phagosome maturation,<sup>29</sup> a mechanism by which pathogens can gain entry. Accordingly, the regulation of PI(4,5)P<sub>2</sub> (and therefore actin polymerization) by OCRL and INPP5B has been implicated in the infectivity of several pathogens, although the specific requirements of OCRL/INPP5B activity varies with the pathogen studied. Depletion of OCRL/INPP5B activity has been linked to a reduction in the inclusion formation of

*chlamydiae*.<sup>30</sup> Similarly, in a genome-wide RNAi screen in *Listeria monocytogenes*, knockdown of OCRL led to decreased entry, reduced vacular escape, and less intracellular growth.<sup>31</sup> The catalytic activity of OCRL and INPP5B has also been implicated in *Yersinia* invasion.<sup>32</sup> Thus, the inhibition of OCRL/INPP5B may be of benefit in protection against pathogen entry.

Concerning other 5-phosphatases, it was reported that decreased levels of synaptojanin 1, a condition that impacts neuronal PI(4,5)P<sub>2</sub>, may have a protective effect on nervous tissue impairment in a mouse model of Alzheimer's disease.<sup>33,34</sup> Furthermore, a chronic steady state decrease of PI(4,5)P<sub>2</sub> levels (due to enhanced expression of synaptojanin 1) may cooperate with the enhanced expression of the A $\beta$  peptide precursor,

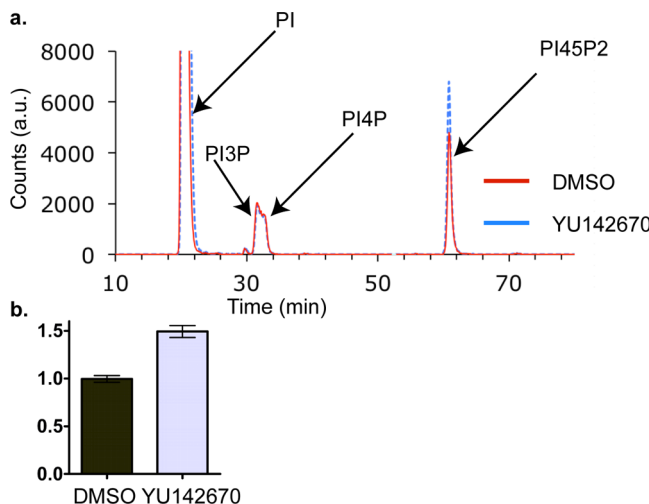


**Figure 6.** Ratio of PI(4,5)P<sub>2</sub> to PI4P levels increase upon treatment of human dermal fibroblasts with 50  $\mu$ M YU142670. Top: representative HPLC run after addition of 0.5% DMSO or YU142670 in 0.5% DMSO showing peaks derived from <sup>3</sup>H-myo-inositol labeled inositol phospholipids. Bottom: quantitation of PI(4)P/PI(4,5)P<sub>2</sub> ration. Error bars indicate standard deviation.

APP, in the onset of early Alzheimer's disease that occurs in all Down's syndrome patients.<sup>35</sup>

Other conditions reflect an absence of specific S-phosphatases, and thus, the design of activators of these enzymes might have more generalized therapeutic value. This could be of benefit, for instance, in the treatment of selected cases of Lowe Syndrome due to destabilizing missense mutations in OCRL that may be rescued by chemical chaperones. More importantly, an activator of OCRL/INPP5B might allow for better compensation of OCRL function by INPP5B, and thus some alleviation of symptoms. Additionally, as PI(4,5)P<sub>2</sub> pools controlled by different S-phosphatases partially overlap, impaired function of a S-phosphatase could be partially rescued by the activation of others.

In summary, our strategy utilizes the major structural classes of this enzyme family, and provides a means for testing substrate selectivity. Additionally, we have identified two novel inhibitor classes that could serve as a starting point for the design of more pharmacologically desirable inhibitors.

## METHODS

**Fluorescence Polarization Assay.** Enzyme (10  $\mu$ L) (see SI Table 2 for final enzyme concentrations) and 10  $\mu$ L of PI(3,4,5)P<sub>3</sub> lipid substrate were added to the assay plate (final concentration of 2.5  $\mu$ M substrate). The reaction was stopped by adding 10  $\mu$ L of detection mix (50 nM GST-TAPP1, 10 nM GloPIPs BODIPY TMR-PI(3,4)P<sub>2</sub>, 20 mM EDTA, final assay concentrations). Fluorescence polarization was read on an Envision plate reader (PerkinElmer) at 531/595 nm excitation/emission.

**Malachite Green Assay.** Enzyme (10  $\mu$ L) (see SI Table 2 for final enzyme concentrations) and 10  $\mu$ L of PI(4,5)P<sub>2</sub> lipid substrate were added to the assay plate (final 25  $\mu$ M substrate). The reaction was stopped by adding 40  $\mu$ L of malachite green solution +0.01% w/v Tween20. Absorbance was read on an Envision plate reader (PerkinElmer) at 620 nm.

**Mobility Shift Assay.** Enzyme (10  $\mu$ L) (see SI Table 2 for final enzyme concentrations) and 10  $\mu$ L of PI(3,4,5)P<sub>3</sub>-fluorescein substrate were added to the assay plate (final concentration of 1  $\mu$ M). Assay plates were incubated for 30 min at RT for hit pick assays, see SI

Table 2 for conditions for dose response curves. The reaction was stopped by adding 1  $\mu$ L of 500 mM EDTA using a MultiChannel Pipettor and heating to 65 °C for 10 min. The shift in electrophoretic mobility caused by removal of the phosphate group from the fluorescent substrate was detected using a LabChip EZReader (Caliper LifeSciences). The percent conversion of substrate to product for each well is calculated from the relative heights of the substrate and product peaks.

## ASSOCIATED CONTENT

### S Supporting Information

Additional tables and figures, detailed methods for protein purification, assay conditions (including a table summarizing all of the reaction conditions used for dose response), methods for isothermal titration calorimetry and cellular assays. This material is available free of charge via the Internet at <http://pubs.acs.org>.

## AUTHOR INFORMATION

### Corresponding Author

\*Phone: 203-737-4461. Fax: 203-737-4436. E-mail: pietro.decamilli@yale.edu.

### Present Addresses

<sup>§</sup>(M.P.) Scholar Rock Inc., 300 Third Street, 4th Floor, Cambridge, MA 02142, United States

<sup>¶</sup>(O.I.-H.) Department of Medical Cell Biology, Uppsala University, 751 05 Uppsala, Sweden

### Notes

The authors declare no competing financial interest.

## ACKNOWLEDGMENTS

We thank D. Hoyer and E. Folta-Stogniew for advice regarding medicinal chemistry and isothermal titration calorimetry (respectively). This work was supported in part by grants from the National Institutes of Health (NIH) (DA018343 and DK082700), the Ellison Foundation, and NARSAD to P.D.C., and a pilot grant awarded to P.D.C. by the Yale Center for Molecular Discovery.

## REFERENCES

- Hakim, S., Bertucci, M. C., Conduit, S. E., Vuong, D. L., and Mitchell, C. A. (2012) Inositol polyphosphate phosphatases in human disease. *Curr. Top. Microbiol. Immunol.* 362, 247–314.
- Wong, K.-K., Engelman, J. A., and Cantley, L. C. (2010) Targeting the PI3K signaling pathway in cancer. *Curr. Opin. Genet. Dev.* 20, 87–90.
- McNamara, C. W., Lee, M. C. S., Lim, C. S., Lim, S. H., Roland, J., Nagle, A., Simon, O., Yeung, B. K. S., Chatterjee, A. K., McCormack, S. L., Manary, M. J., Zeeman, A.-M., Dechering, K. J., Kumar, T. R. S., Henrich, P. P., Gagaring, K., Ibanez, M., Kato, N., Kuhen, K. L., Fischli, C., Rottmann, M., Plouffe, D. M., Bursulaya, B., Meister, S., Rameh, L., Trappe, J., Haasen, D., Timmerman, M., Sauerwein, R. W., Suwanarusk, R., Russell, B., Renia, L., Nosten, F., Tully, D. C., Kocken, C. H. M., Glynne, R. J., Bodenreider, C., Fidock, D. A., Diagana, T. T., and Winzeler, E. A. (2013) Targeting Plasmodium PI(4)K to eliminate malaria. *Nature* 504, 248–253.
- Cai, X., Xu, Y., Cheung, A. K., Tomlinson, R. C., Alcázar-Román, A., Murphy, L., Billlich, A., Zhang, B., Feng, Y., Klumpp, M., Rondeau, J.-M., Fazal, A. N., Wilson, C. J., Myer, V., Joberty, G., Bouwmeester, T., Labow, M. A., Finan, P. M., Porter, J. A., Ploegh, H. L., Baird, D., de Camilli, P., Tallarico, J. A., and Huang, Q. (2013) PIKfyve, a class III PI kinase, is the target of the small molecular IL-12/IL-23 inhibitor apilimod and a player in Toll-like receptor signaling. *Chem. Biol.* 20, 912–921.

- (5) McIntire, L. B. J., Lee, K.-I., Chang-Ikleo, B., Di Paolo, G., and Kim, T.-W. (2013) Screening assay for small-molecule inhibitors of Synaptojanin 1, a synaptic phosphoinositide phosphatase. *J. Biomol Screen.* 19, 585–594.
- (6) Kim, W. T., Chang, S., Daniell, L., Cremona, O., Di Paolo, G., and de Camilli, P. (2002) Delayed reentry of recycling vesicles into the fusion-competent synaptic vesicle pool in synaptojanin 1 knockout mice. *Proc. Natl. Acad. Sci. U.S.A.* 99, 17143–17148.
- (7) Pirruccello, M., and de Camilli, P. (2012) Inositol 5-phosphatases: insights from the Lowe syndrome protein OCRL. *Trends Biochem. Sci.* 37, 134–143.
- (8) Ooms, L. M., Horan, K. A., Rahman, P., Seaton, G., Gurung, R., Kethesparan, D. S., and Mitchell, C. A. (2009) The role of the inositol polyphosphate 5-phosphatases in cellular function and human disease. *Biochem. J.* 419, 29–49.
- (9) Laxminarayan, K. M., Matzaris, M., Speed, C. J., and Mitchell, C. A. (1993) Purification and characterization of a 43-kDa membrane-associated inositol polyphosphate 5-phosphatase from human placenta. *J. Biol. Chem.* 268, 4968–4974.
- (10) Ong, C. J., Ming-Lum, A., Nodwell, M., Ghanipour, A., Yang, L., Williams, D. E., Kim, J., Demirjian, L., Qasimi, P., Ruschmann, J., Cao, L.-P., Ma, K., Chung, S. W., Duronio, V., Andersen, R. J., Krystal, G., and Mui, A. L.-F. (2007) Small-molecule agonists of SHIP1 inhibit the phosphoinositide 3-kinase pathway in hematopoietic cells. *Blood* 110, 1942–1949.
- (11) Brooks, R., Fuhler, G. M., Iyer, S., Smith, M. J., Park, M.-Y., Paraiso, K. H. T., Engelman, R. W., and Kerr, W. G. (2010) SHIP1 inhibition increases immunoregulatory capacity and triggers apoptosis of hematopoietic cancer cells. *J. Immunol.* 184, 3582–3589.
- (12) Suwa, A., Yamamoto, T., Sawada, A., Minoura, K., Hosogai, N., Tahara, A., Kurama, T., Shimokawa, T., and Aramori, I. (2009) Discovery and functional characterization of a novel small molecule inhibitor of the intracellular phosphatase, SHIP2. *Br. J. Pharmacol.* 158, 879–887.
- (13) Rowe, T., Hale, C., Zhou, A., Kurzeja, R. J. M., Ali, A., Menjares, A., Wang, M., and McCarter, J. D. (2006) A high-throughput microfluidic assay for SH2 domain-containing inositol 5-phosphatase 2. *Assay Drug Dev Technol.* 4, 175–183.
- (14) Cremona, O., Di Paolo, G., Wenk, M. R., Luthi, A., Kim, W. T., Takei, K., Daniell, L., Nemoto, Y., Shears, S. B., Flavell, R. A., McCormick, D. A., and de Camilli, P. (1999) Essential role of phosphoinositide metabolism in synaptic vesicle recycling. *Cell* 99, 179–188.
- (15) McPherson, P. S., Garcia, E. P., Slepnev, V. I., David, C., Zhang, X., Grabs, D., Sossin, W. S., Bauerfeind, R., Nemoto, Y., and de Camilli, P. (1996) A presynaptic inositol-5-phosphatase. *Nature* 379, 353–357.
- (16) Drees, B. E., Weipert, A., Hudson, H., Ferguson, C. G., Chakravarty, L., and Prestwich, G. D. (2003) Competitive fluorescence polarization assays for the detection of phosphoinositide kinase and phosphatase activity. *Comb. Chem. High Throughput Screening* 6, 321–330.
- (17) Tsujishita, Y., Guo, S., Stoltz, L. E., York, J. D., and Hurley, J. H. (2001) Specificity determinants in phosphoinositide dephosphorylation: Crystal structure of an archetypal inositol polyphosphate 5-phosphatase. *Cell* 105, 379–389.
- (18) Trésaguet, L., Silvander, C., Flodin, S., Welin, M., Nyman, T., Gräslund, S., Hammarström, M., Berglund, H., and Nordlund, P. (2014) Structural basis for phosphoinositide substrate recognition, catalysis, and membrane interactions in human inositol polyphosphate 5-phosphatases. *Structure*, DOI: 10.1016/j.str.2014.01.013.
- (19) Zhang, X., Jefferson, A. B., Auethavekiat, V., and Majerus, P. W. (1995) The protein deficient in Lowe syndrome is a phosphatidylinositol-4,5-bisphosphate 5-phosphatase. *Proc. Natl. Acad. Sci. U.S.A.* 92, 4853–4856.
- (20) Schmid, A. C., Wise, H. M., Mitchell, C. A., Nussbaum, R., and Woscholski, R. (2004) Type II phosphoinositide 5-phosphatases have unique sensitivities towards fatty acid composition and head group phosphorylation. *FEBS Lett.* 576, 9–13.
- (21) Suchy, S. F., and Nussbaum, R. L. (2002) The deficiency of PIP2 5-phosphatase in Lowe syndrome affects actin polymerization. *Am. J. Hum. Genet.* 71, 1420–1427.
- (22) Cui, S., Guerriero, C. J., Szalinski, C. M., Kinlough, C. L., Hughey, R. P., and Weisz, O. A. (2010) OCRL1 function in renal epithelial membrane traffic. *Am. J. Physiol. Renal Physiol.* 298, F335–F345.
- (23) Vicinanza, M., Di Campli, A., Polishchuk, E., Santoro, M., Di Tullio, G., Godi, A., Levchenko, E., De Leo, M. G., Polishchuk, R., Sandoval, L., Marzolo, M., and De Matteis, M. A. (2011) OCRL controls trafficking through early endosomes via PtdIns4,5P(2)-dependent regulation of endosomal actin. *EMBO J.* 30, 4970–4985.
- (24) Takenawa, T., and Itoh, T. (2001) Phosphoinositides, key molecules for regulation of actin cytoskeletal organization and membrane traffic from the plasma membrane. *Biochim. Biophys. Acta* 1533, 190–206.
- (25) Burkel, B. M., Dassow, von, G., and Bement, W. M. (2007) Versatile fluorescent probes for actin filaments based on the actin-binding domain of utrophin. *Cell Motil. Cytoskeleton* 64, 822–832.
- (26) Idevall-Hagren, O., Dickson, E. J., Hille, B., Toomre, D. K., and de Camilli, P. (2012) Optogenetic control of phosphoinositide metabolism. *Proc. Natl. Acad. Sci. U.S.A.* 109, E2316–E2323.
- (27) Pizarro-Cerdá, J., and Cossart, P. (2004) Subversion of phosphoinositide metabolism by intracellular bacterial pathogens. *Nat. Cell Biol.* 6, 1026–1033.
- (28) Erdmann, K. S., Mao, Y., McCrea, H. J., Zoncu, R., Lee, S., Paradise, S., Modregger, J., Biemesderfer, D., Toomre, D., and de Camilli, P. (2007) A role of the Lowe syndrome protein OCRL in early steps of the endocytic pathway. *Dev. Cell* 13, 377–390.
- (29) Bohdanowicz, M., Balkin, D. M., de Camilli, P., and Grinstein, S. (2012) Recruitment of OCRL and InppSB to phagosomes by Rab5 and APPL1 depletes phosphoinositides and attenuates Akt signaling. *Mol. Biol. Cell* 23, 176–187.
- (30) Moorhead, A. M., Jung, J.-Y., Smirnov, A., Kaufer, S., and Scidmore, M. A. (2010) Multiple host proteins that function in phosphatidylinositol-4-phosphate metabolism are recruited to the chlamydial inclusion. *Infect. Immun.* 78, 1990–2007.
- (31) Cheng, L. W., Viala, J. P. M., Stuurman, N., Wiedemann, U., Vale, R. D., and Portnoy, D. A. (2005) Use of RNA interference in *Drosophila* S2 cells to identify host pathways controlling compartmentalization of an intracellular pathogen. *Proc. Natl. Acad. Sci. U.S.A.* 102, 13646–13651.
- (32) Sarantis, H., Balkin, D. M., de Camilli, P., Isberg, R. R., Brumell, J. H., and Grinstein, S. (2012) Yersinia entry into host cells requires Rab5-dependent dephosphorylation of PI(4,5)P<sub>2</sub> and membrane scission. *Cell Host Microbe* 11, 117–128.
- (33) Berman, D. E., Dall'Armi, C., Voronov, S. V., McIntire, L. B., Zhang, H., Moore, A. Z., Staniszewski, A., Arancio, O., Kim, T. W., and Di Paolo, G. (2008) Oligomeric amyloid- $\beta$  peptide disrupts phosphatidylinositol-4,5-bisphosphate metabolism. *Nat. Neurosci.* 11, 547–554.
- (34) McIntire, L. B. J., Berman, D. E., Myaeng, J., Staniszewski, A., Arancio, O., Di Paolo, G., and Kim, T.-W. (2012) Reduction of synaptojanin 1 ameliorates synaptic and behavioral impairments in a mouse model of Alzheimer's disease. *J. Neurosci.* 32, 15271–15276.
- (35) Voronov, S. V., Frere, S. G., Giovedi, S., Pollina, E. A., Borel, C., Zhang, H., Schmidt, C., Akeson, E. C., Wenk, M. R., Cimasoni, L., Arancio, O., Davisson, M. T., Antonarakis, S. E., Gardiner, K., de Camilli, P., and Di Paolo, G. (2008) Synaptojanin 1-linked phosphoinositide dyshomeostasis and cognitive deficits in mouse models of Down's syndrome. *Proc. Natl. Acad. Sci. U.S.A.* 105, 9415–9420.